Mechanics of Advanced Composite Structures 7(2020) 321 - 331

Semnan University

Mechanics of Advanced Composite Structures

journal homepage: http://MACS.journals.semnan.ac.ir

Size-Dependent Nonlinear Dynamics of a Non-Uniform Piezoelectric Microbeam Based on the Strain Gradient Theory

A. Feyz Sayadian, S. Faroughi *

Faculty of Mechanical Engineering, Urmia University of Technology, Urmia, Iran

KEYWORDS

Piezoelectric
Microbeam
strain gradient theory
Nonlinear geometry
Primary resonance
Sub/super harmonic

ABSTRACT

In this research, the nonlinear dynamics of an electrostatically actuated non-uniform microbeam equipped with a damping film and a piezoelectric layer have been studied. The nonlinear behaviour of the system was modelled using the von Karman geometrical strain terms. In addition, the strain gradient theory was utilized and the Hamilton principle was applied to obtain equations of motion and boundary conditions, respectively. The obtained equations were reduced using the Galerkin method, and the reduced equations were solved with the multiple scale method. The size-dependent responses were then investigated for primary, super-harmonic, and sub-harmonic resonances. The influence of beam width, beam thickness, and distance between electrodes on the resonant frequency response was studied along with nonlinearity of the system. The results showed that the static and forced vibration behaviours of microbeams strongly depended on the size of the electrodes.

1. Introduction

Nano electromechanical sensors and Micro electromechanical sensors (NEMS and MEMS) are considered a potential alternative to mechanical sensors for improving the sensitivity, lowering power consumption, and widening the bandwidths of conventional resistance strain gauges. Furthermore, design and manufacturing problems at the micron level has been an important challenge during the last decades, because the size of a MEMS structure is in a range of lower than 10 microns. For instance, the thickness of the thin piezoelectric film is about less than 1 micron, and the particle size of an advanced admixture is about 1 micron.

Therefore, notable researches have been conducted about static and dynamic characteristics of micro sized structures, such as microbeams, microfilms, and micro actuators, including a vast amount of attention paid recently to research and studies related to statics and dynamics of micro-sized structures, such as microbeams, microfilms, and microactuators [1].

In the recent years, mathematical modelling of the mechanical behaviour of MEMS and NEMS has been of great interest to researchers. Since, microbeams have been widely used in many instruments, such as vibration shock sensors, electrostatic actuators, and atomic microscopes. Additionally, micro-scaled gadgets which consume energy in microwatts need a small amount of operation power, therefore harvesting energy from the surrounding environment can be a significant source of power for such structures[2]. There are various environmental sources of energy, such as light, heat and mechanical vibration. Moreover, there usually exists a notable amount of mechanical energy in our surroundings in the form of mechanical vibrations that can be considered as an important energy source among other sources. As a result, by using an electromechanical converter, this surrounding source of energy can be transmuted into useful electrical energy [3].

Different instruments such as electromagnetic, piezoelectric, and electrostatic transducers can be used for transmuting mechanical energy into electrical energy. It can be stated that, piezoelectric and electrostatic transducers are the most commonly used tools for application in MEMS scale harvesters because of their viability.

*Corresponding author. Tel.: +98-9185676324.
E-mail address: sh.farughi@uut.ac.ir

DOI: 10.22075/MACS.2020.18013.1210
Received 2019-06-10; Received in revised form 2019-11-13; Accepted 2020-02-07
© 2020 Published by Semnan University Press. All rights reserved.

Electrostatic actuation is also one of the most commonly applied methods for inspecting microscale gadgets. A flexible distortable beam over a firm substrate, parted by an actuated electrostatically dielectric embedded medium is a regular device used in this field. As the mentioned beam is actuated by electrostatic forces, it bends and turns toward the still electrode. At this moment, because of the flexible reinstating force restriction, the beam tends to go back to its initial position where it is not deformed [4].

Younis [5] investigated the static and dynamic behaviours of electrostatically actuated microbeam-based MEMS suggesting a logical technique similar to a reduced-order macromodel. Abdel-Rahman et al [6] introduced a reduced-order macromodel to estimate the dynamic behaviours of electrostatically actuated microbeam-based MEMS . Kivi et al. [7] studied the nonlinear size-dependent static and dynamic behaviours of an electrostatically actuated nano-beam. The investigated deformable electrode was considered as a completely clamped nano-beam in NEMS. Ghayesh et al[8] also studied the nonlinear size-dependent behaviour of an electrostatically actuated Micro electromechanical systems resonator based on the couple stress theory.

On the other hand, there are major drawbacks of using a microbeam for electrostatic actuation. Therefore, using piezoelectric components in micro devices can be an ideal alternative because of lightness, fastness of response, wideness of bandwidth, and low power consumption. Moreover, the properties of theses piezoelectric materials make them suitable for using both in sensors and actuators in micro or nano-scale structures.[9]

Ghorbanpour et al [9] analysed a piezoelectric nanobeam in a nonlinear vibration situation with the strain gradient theory. Ansari [10] conducted another study about vibrational characteristics of piezoelectric microbeams based on the modified theory of stress couple. Hosseini [11] studied the nonlinear forced vibrations of a microbeam with a piezoelectric layer on its top surface through the Multiple Scales method. Chorsi et al [12] examined the nonlinear dynamics of a two-sided capacitive micro-beam under electrostatic actuation. Since, the piezoelectric actuation imposes a longitudinal axial force to the micro-beam that shifts the primary resonance of the micro resonator, therefore it can be used as a tuning tool.

Because of their electromechanical coupling capabilities, piezoelectric materials have a fast responding nature. Although piezoelectric materials can be extremely beneficial in controlling the structural behaviours of electromechanical systems, they have not been perpended much by the researchers so far. Therefore, creating an axial force in the structure for achieving higher efficiency appears to be a formidable concept in the design and improvement of such structures. So, producing axial force in microstructures in order to get higher efficiency could lead to new ideas in designing and improving structures using piezoelectric actuation, so that both electrostatic and piezoelectric materials could be used for increasing safety factors [5].

Chitsaz Yazdi [13] presented an analysis for static and dynamic reactions of a clamped–clamped nanocomposite microbeam with electrostatic and piezoelectric actuations. The governing equations of motion were obtained through the Hamilton principle in this research. Khodaparast [14] presented a piezoelectric vibration based energy harvesting system with the use of an electrostatic device. Controlling the resonance frequency of the piezoelectric harvester with DC voltages applied to the electrostatic system for maximizing the harvested power, was the main objective of their study. The idea was implemented as a hybrid system including a cantilevered piezoelectric harvester, an electrostatic harvester, and a variable voltage source. Hoshiar et al. [15] also presented a nonlinear analysis for a micro-system under piezoelectric and electrostatic actuations.

Because of the lack of size related parameters in the constitutive correlations of microstructures, classical flexible theories have not been able to explain the effects of size on material properties. Therefore, finding a theoretical model forming a quantitative relationship between the material's microstructure and macromechanical properties seems to be necessary. Recently, modelling of MEMS structures and devices with size dependant continuum mechanics theories has received an increasing attention particularly regarding some higher-order continuums.

Moreover, the size-dependent behaviour that takes place in sub-micron and micron scales cannot be predicted and explained by the classic continuum mechanics theories. However, the size-dependent behaviour can acceptably be considered by some non-classical continuum theories such as the higher-order gradient and couple stress theories. The higher-order gradient and couple stress theories can acceptably take the size-dependent parameters into account. In the 1960s many researchers like Touplin and Koiter [16] presented the modified theory of couple stress proposing the use of two high-order material length scale parameters in the constitutive predicaments besides the two classical constants of Lame. As some previously used implementations, this theory was used by Zhou and Li [17] for examination and inspection of both the static and dynamic behaviour of a micro-bar in torsion. In addition, some other

examinations were conducted by Asghari et al [18]. Yang et al [19] also used the size-dependent modified couple stress theory for the modelling of Timoshenko beams. The additional predicament in this study was the motion of the coupled equation. Moreover, the couple stress theories constitutive predicaments were modified and new constitutive predicaments were presented with only one material length scale parameter.

Assuming that the continuum's strain energy density does not solely depend on the strain, but on the strain tensor's first spatial derivative as well, Fleck and Hutchinson [20] presented a strain gradient theory in which five higher-order material constants were brought into the constitutive predicaments of the continuum. Later, Lam et al [21] offered a modified strain gradient theory based on the modified couple stress theory depending on three lone higher-order material constants disregarding additional higher-order terms.

The large deflection forced vibrations of a rectangular uniform cross-sectional microbeam was analysed by Kahrobaiyan using the perturbation technique [22]. Yonus and Nayfe [23] presented a nonlinear model for analysing electrostatic micro-beams including the stored force in a microbeam.

In this current study, the main activity was to employ both piezoelectric and electrostatic excitations for analysing the feasibility of their applications. The size-dependent nonlinear dynamics of a non-uniform piezoelectric microbeam were studied based on the strain gradient theory. The strain gradient theory was used in this study because of its high accuracy. This work also employed the multiple scale method to study nonlinear dynamics of a non-uniform piezoelectric microbeam such as primary, sub-harmonic and super-harmonic resonances.

2. The Strain gradient theory

The studied model was a non-uniform microbeam that was coated by a piezoelectric layer illustrated in Fig. 1. A non-uniform microbeam with length (L), thickness (h), width (b), $E_b$and E_p were the elasticity modulus of the microbeam and the piezoelectric layers, h_p and $h_b$were the thickness of the piezoelectric layer and microbeam, respectively. The total height of the micro-beam was $h = h_p + h_b$. A density ρ_p and piezoelectric coefficient equivalent to e_{31}, g_0 was the initial gap between the microbeam and the stationary electrode. The vacuum gap had the permittivity of the vacuum piezoelectric coefficient equivalent to ε_v. A voltage (V) was applied to the beam while a voltage (V_p) was applied to the piezoelectric layer.

In addition, the strain gradient elasticity theory, proposed in 2003 by Lam et al. [22], was more comprehensively compared to the modified couple stress theory. According to the strain gradient theory, U is the energy density in a tensor (bound with stress regarding force) and symmetric curvature tensor (bound with stress regarding coupling) function. The strain energy U for a homogeneous deformed matter in the domain Ω is as follows: [24]

$$U = \frac{1}{2}\iiint_{\Omega}\left(\sigma_{ij}\varepsilon_{ij} + p_i\gamma_i + \tau_{ijk}^{(1)}\eta_{ijk}^{(1)} + m_{ij}^{s}\chi_{ij}^{s}\right) d\Omega \quad (1)$$

Where Ω in the occupied region and ε, σ, χ, m is Classical strain tensor, Cauchy stress Deviation part of couple stress and Symmetric curvature, respectively. The terms of the (1) are defined as follows[19]:

$$\gamma_i = \varepsilon_{mm,i} \quad (2)$$

$$\eta_{ijk}^{(1)} = \frac{1}{3}\left(\varepsilon_{jk,i} + \varepsilon_{ki,j} + \varepsilon_{ij,k}\right) - \frac{1}{15}\delta_{ij}\left(\varepsilon_{mm,k} + 2\varepsilon_{mk,m}\right) - \frac{1}{15}\left[\delta_{jk}\left(\varepsilon_{mm,i} + 2\varepsilon_{mi,m}\right) + \delta_{ki}\left(\varepsilon_{mm,j} + 2\varepsilon_{mj,m}\right)\right] \quad (3)$$

$$\sigma_{ij} = \lambda\varepsilon_{mm}\delta_{ij} + 2G\varepsilon_{ij} \quad (4)$$

$$m_{ij}^{s} = 2\mu l_2^2\chi_{ij}^{s} \qquad i,j = 1,2,3 \quad (5)$$

$$\varepsilon_{ij} = \frac{1}{2}\left(\partial_i u_j + \partial_j u_i\right) \quad (6)$$

$$\chi_{ij} = \frac{1}{2}\left(\partial_i\theta_j + \partial_j\theta_i\right) \quad (7)$$

$$p_i = 2\mu l_0^2\gamma_i \quad (8)$$

$$\tau_{ijk}^{(1)} = 2\mu l_1^2\eta_{ijk}^{(1)} \quad (9)$$

In which u and θ are the displacement and rotary vectors, respectively. The u_x, u_y and u_z are displacements along the x, y and z axes of the beam and are introduced as follow:

$$u_x(x,z,t) = -z\frac{\partial w}{\partial x}\ , u_y(x,z,t) = 0,\ u_z(x,z,t) = w(x,t) \quad (10)$$

The relations ε for the microbeam can be obtained by using (11):

$$\varepsilon_{xx} = -z\frac{\partial^2 w}{\partial x^2} + \frac{1}{2}\left(\frac{\partial w}{\partial x}\right)^2, \varepsilon_{zz} = 0, \varepsilon_{xy} = \varepsilon_{yx} = \varepsilon_{zy} = \varepsilon_{yz} = \varepsilon_{xz} = \varepsilon_{zx} = 0 \quad (11)$$

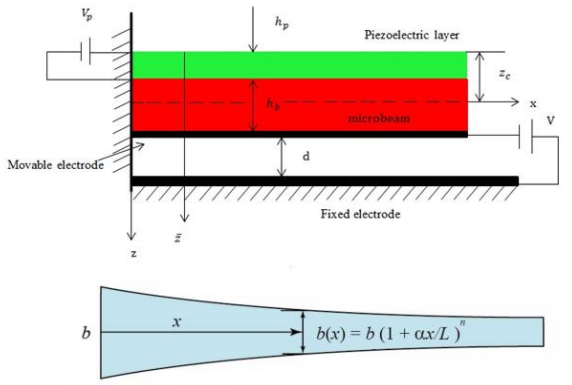

Fig. 1. Schematic image of an electrostatically actuated microbeam with piezoelectric layer

Also, the relations of θ for the Euler-Bernoulli beam can be estimated by using the following equation:

$$\theta = \frac{1}{2} curl(u) \tag{12}$$

$$\theta_y = -\frac{\partial w}{\partial x}, \theta_x = \theta_z = 0 \tag{13}$$

$$\eta_{111}^{(1)} = \frac{\partial \varepsilon_{11}}{\partial x} = \eta_{111}^{(1)} = \frac{2}{5}\left(-z\frac{\partial^3 w}{\partial x^3} + \frac{\partial w}{\partial x}\frac{\partial^2 w}{\partial x^2}\right) \tag{14}$$

$$\eta_{113}^{(1)} = \eta_{131}^{(1)} = \eta_{311}^{(1)} = \frac{4}{15}\left(-\frac{\partial^2 w}{\partial x^2}\right) \tag{15}$$

$$\eta_{122}^{(1)} = \eta_{133}^{(1)} = \eta_{212}^{(1)} = \eta_{221}^{(1)} = \eta_{313}^{(1)} = \eta_{331}^{(1)} = -\frac{1}{5\left(\frac{\partial w \partial^2 w}{\partial x \partial x^2} - z\frac{\partial^3 w}{\partial x^3}\right)} \tag{16}$$

$$\eta_{223}^{(1)} = \eta_{232}^{(1)} = \eta_{322}^{(1)} = \frac{1}{15}\left(\frac{\partial^2 w}{\partial x^2}\right) \tag{17}$$

$$\eta_{333}^{(1)} = \frac{1}{5}\left(\frac{\partial^2 w}{\partial x^2}\right) \tag{18}$$

$$p_1 = 2\mu l_0^2 \left(\frac{\partial w}{\partial x}\frac{\partial^2 w}{\partial x^2} - z\frac{\partial^3 w}{\partial x^3}\right) \tag{19}$$

$$p_3 = -2\mu l_0^2 \left(\frac{\partial^2 w}{\partial x^2}\right) \tag{20}$$

$$m_{12} = m_{21} = -\frac{\mu l_2^2}{2}\left(\frac{\partial^2 w}{\partial x^2}\right) \tag{21}$$

$$\gamma_x = -z\frac{\partial^3 w}{\partial x^3} + \frac{\partial w}{\partial x}\frac{\partial^2 w}{\partial x^2} \tag{22}$$

$$\gamma_z = -\frac{\partial^2 w}{\partial x^2} \tag{23}$$

$$\chi_{xy}^{(s)} = \chi_{yx}^{(s)} = -\frac{1}{4}\left(\frac{\partial^2 w}{\partial x^2}\right) \tag{24}$$

$$\tau_{111}^{(1)} = \frac{4}{5}\mu l_1^2 \left(\frac{\partial w}{\partial x}\frac{\partial^2 w}{\partial x^2} - z\frac{\partial^3 w}{\partial x^3}\right) \tag{25}$$

$$\tau_{113}^{(1)} = \tau_{131}^{(1)} = \tau_{311}^{(1)} = \frac{8}{15}\mu l_1^2 \left(-\frac{\partial^2 w}{\partial x^2}\right) \tag{26}$$

$$\tau_{122}^{(1)} = \tau_{133}^{(1)} = \tau_{212}^{(1)} = \tau_{221}^{(1)} = \tau_{313}^{(1)} = \tau_{331}^{(1)} = -\frac{2}{5}\mu l_1^2 \left(\frac{\partial w}{\partial x}\frac{\partial^2 w}{\partial x^2} - z\frac{\partial^3 w}{\partial x^3}\right) \tag{27}$$

$$\tau_{223}^{(1)} = \tau_{232}^{(1)} = \tau_{322}^{(1)} = \frac{2}{15}\mu l_1^2 \left(\frac{\partial^2 w}{\partial x^2}\right) \tag{28}$$

$$\tau_{333}^{(1)} = \frac{2}{5}\mu l_1^2 \left(\frac{\partial^2 w}{\partial x^2}\right) \tag{29}$$

The non-zero stresses σ_{ij} of the microbeam that can be obtained as:

$$\sigma_{xx} = E\varepsilon_{xx} = E(z)\varepsilon_{xx} \tag{30}$$

For the piezoelectric layer, stress tensor is:

$$\sigma_{xx} = E\left(\frac{1}{2}\left(\frac{\partial w}{\partial x}\right)^2 - z\frac{\partial^2 w}{\partial x^2}\right) - e_{31}E_z = E(z)\varepsilon_{xx} - e_{31}E_z \tag{31}$$

In (31), the ε has strained the cross-section of the system while the e_{31}remains constant in the piezoelectric layer. Also $E_z = \frac{V_p}{h_p}$.

Substituting the (13-31) in (1) and integrating on the volume of the micro beam, the total strain energy for the microbeam is calculated as:

$$U_1 = \int_0^L \int_A \left(\sigma_{ij}\varepsilon_{ij} + p_i\gamma_i + \tau_{ijk}^{(1)}\eta_{ijk}^{(1)} + m_{ij}^{(s)}\chi_{ij}^{(s)}\right)dAdx = \frac{1}{2}\int_0^L \int_A \left\{E\left[\frac{1}{2}\left(\frac{\partial w}{\partial x}\right)^2 - z\frac{\partial^2 w}{\partial x^2}\right]^2 + 2\mu l_0^2\left(\frac{\partial^2 w}{\partial x^2}\right)^2 + \left(2\mu l_0^2 + \frac{4}{5}\mu l_1^2\right)\left(\frac{\partial w}{\partial x}\frac{\partial^2 w}{\partial x^2} - z\frac{\partial^4 w}{\partial x^4}\right)^2 + \frac{8}{15}\mu l_1^2\left(-\frac{\partial^2 w}{\partial x^2}\right)\right\}dAdx \tag{32}$$

The kinetic energy for the microbeam is also obtained as follows:

$$T = \frac{1}{2}\int_0^L \left\{m\left(\frac{\partial w}{\partial x}\right)\right\}dx \tag{33}$$

Where m is the linear density of the microbeam defined by:

$$m = \rho_p A_p(x) + \rho_b A_b(x) \tag{34}$$

Due to the piezoelectric actuation force, the strain energy for the piezoelectric layer can also be calculated as:

$$U_p = \frac{1}{2}\int_0^L \left\{N_{0x}\left(\frac{\partial w}{\partial x}\right)^2\right\}dx \tag{35}$$

The parameter N_{0x} is:

$$N_{0x} = -be_{31}V_0 \tag{36}$$

Considering the relations between T and U, by applying the Hamilton principle the governing equation of the microbeam can be achieved based on the strain gradient theory. The Hamilton principal can be estimated by using the following equation:

$$U = \frac{1}{2}\int_0^L \Big((EI)_{eq} + 2(\mu Al_0^2)_{eq} + \frac{8}{15}(\mu Al_1^2)_{eq} + (\mu Al_2^2)_{eq}\Big)\left(\frac{\partial^2 w}{\partial x^2}\right)^2 + \Big(2(\mu Il_0^2)_{eq} + \frac{4}{5}(\mu Il_1^2)_{eq}\Big)\left(\frac{\partial^3 w}{\partial x^3}\right)^2 + \frac{1}{2}(EA)_{eq}\left(\frac{\partial w}{\partial x}\right)^4 + \Big(2(\mu Al_0^2)_{eq} + \frac{4}{5}(\mu Al_1^2)_{eq}\Big)\left(\frac{\partial w}{\partial x}\right)^2\left(\frac{\partial^2 w}{\partial x^2}\right)^2 + \Big(4(\mu Al_0^2)_{eq} + \frac{8}{5}(\mu Al_1^2)_{eq}\Big)\left(\frac{\partial w}{\partial x}\right)\left(\frac{\partial^2 w}{\partial x^2}\right)\left(\frac{\partial^3 w}{\partial x^3}\right) \tag{37}$$

$$T = \frac{1}{2}\int_0^L m\left(\frac{\partial w}{\partial t}\right)^2 dx \tag{38}$$

In this paper A and I were obtained with (39):

$$\begin{cases} \mathrm{A(x)} = \mathrm{A_0}\left(1 + \alpha\left(\frac{\mathrm{x}}{\mathrm{L}}\right)^{\mathrm{i}}\right) \\ \mathrm{I(x)} = \mathrm{I_0}\left(1 + \alpha\left(\frac{\mathrm{x}}{\mathrm{L}}\right)^{\mathrm{i}}\right) \end{cases} \tag{39}$$

For considering the system with the electrostatic actuation and the squeeze-film damping, ($p = p_e + p_c$), was used, where $\mathrm{p_e}$ is the electrostatically actuated force and $\mathrm{p_c}$ is the squeeze film damping force. According to the conditions of the piezoelectric micro-beam and the electrode, these applied forces are written as follows:

$$p_e = \frac{\varepsilon_0 b Z^2(t)}{2(d-w)^2} \ , \ p_c = -\frac{c_s b^3}{(d-w)^3}\dot{w} \tag{40}$$

In (40), Z(t) is the applied voltage, ε_0 is the vacuum permittivity and $\mathrm{c_s}$ is the viscosity coefficient of the air. For the AC voltage, we have:

$$Z^2(t) = [v_{ac}\cos(\omega t)]^2 = \frac{1}{2}v_{ac}^2[1 + \cos(2\omega_0 t)] \tag{41}$$

Then, the variation of the work done by the external forces is:

$$\delta W = \int_0^L F(x,t)\delta w dx \tag{42}$$

The equation of motion can be obtained by using the Hamiltonian principle:

$$\int_{t1}^{t2}(\delta T - \delta U + \delta W)dt = 0 \tag{43}$$

The equation of motion is as follow:

$$be_{31} \tag{44}$$

The boundary conditions are:

$$w(0,t) = w(L,t) = w''(0,t) = w''(L,t) = 0 \tag{45}$$

To transform the equations of motion and boundary conditions to the dimensionless state, after obtaining the equations of motion and boundary conditions, we made them non-dimensional (Appendix1) .

3. Forced Vibration Analysis

In this section, the forced vibration of the microbeam is studied by using the multiple scales method. To solve this, the original PDE can be converted to an ODE. In order to obtain the mode shapes of the microbeam using Galerkin's method the equations are:

$$W(X,\tau) = \varphi(X)S(\tau) \tag{46}$$

Where $\varphi(X)$ is the first mode shape and S(τ) is the time dependent function. Therefore, we have:

$$\ddot{S} + k_1 S = \varepsilon\big[k_2\cos(\Omega\tau) + k_3 S\text{-}\cos(\Omega\tau) - k_4 S^3 - k_5\dot{S}\big] \tag{47}$$

Where ε is a small non-dimensional parameter. The multiple scale method was used to approach an approximate solution of the domain of the equation. The solution of the homogeneous section of equation (47) is as follows:

$$S(\tau) = Y_1(T_0,T_1) + \varepsilon Y_2(T_0,T_1) \tag{48}$$

$T_n = \varepsilon^n\tau, n = 0{,}1$ and also, $\varepsilon \ll 1$, which is a non-dimensional parameter, small and positive and represents the order of the equations. We have:

$$\begin{aligned} &(\partial\text{^}2\ Y\_1)/(\partial T\_0\text{^}2\ ) + \varepsilon\ (\partial\text{^}2\ Y\_2)/(\partial T\_0\text{^}2\ ) + 2\varepsilon\ (\partial\text{^}2\ Y\_1)/(\partial T\_0\ \partial T\_1\ ) + 2\varepsilon\text{^}2\ \ (\partial\text{^}2\ Y\_2)/(\partial T\_0\ \partial T\_1\ ) + \varepsilon\text{^}2\ ((\partial\text{^}2\ Y\_1)/(\partial T\_0\ \partial T\_2\ ) + 2\varepsilon\ (\partial\text{^}2\ Y\_2)/(\partial T\_0\ \partial T\_2\ ) + (\partial\text{^}2\ Y\_1)/(\partial T\_1\text{^}2\ ) + \varepsilon\ (\partial\text{^}2\ Y\_2)/(\partial T\_1\text{^}2\ ) + k\_1\ (Y\_1 + \varepsilon Y\_2\ ) = \varepsilon[k\_2\ \cos\ (\Omega\tau) + k\_3\ (Y\_1 + \varepsilon Y\_2\ )\ \cos\ (\Omega\tau) - k\_4\ (Y\_1 + \varepsilon Y\_2\ )\text{^}3 - k\_5\ ((\partial Y\_1)/(\partial T\_0\ ) + \varepsilon\ (\partial Y\_2)/(\partial T\_0\ ) + \varepsilon\ (\partial Y\_1)/(\partial T\_1\ ) + \varepsilon\text{^}2\ \ (\partial Y\_1)/(\partial T\_2\ ) + \varepsilon\text{^}3\ \ (\partial Y\_2)/(\partial T\_2\ ) + \cdots) \end{aligned} \tag{49}$$

So, equally replacing equal powers of ε on both sides of the equation, the equations are as follows:

$$\begin{aligned} &\varepsilon^0 : D_0^2 Y_1 + k_1 Y_1 = 0, \\ &\varepsilon^1 : D_0^2 Y_2 + k_1 Y_2 = -2D_0^1 D_1^1 Y_1 + k_2\cos(\Omega\tau) + k_3\cos(\Omega\tau)Y_1 - k_4 Y_1^3 - \end{aligned} \tag{50}$$

$k_5 D_0^1 Y_1$

The solution of equation (49) can be considered as follows:

$$Y_1 = A(T_1)\, exp(ipT_0) + cc \tag{51}$$

The value of $A(T_1) is$ in (51) as follows:

$$A(T_1) = \frac{1}{2} a\, exp(i\beta) \tag{52}$$

A is a function of T_1 and cc represents conjugate terms in (51), and $A(T_1)$ is a complex function. Note that p^2=k_1 and substituting (52) in (50):

$$\begin{aligned} &D\_0\text{^}2\, Y\_2 + p\text{^}2\, Y\_2 = \\ &-2ipD\_1\text{^}1\, A(T\_1)\ exp\ (ipT\_0) + \\ &1/2\ k\_2\ cos\ (\Omega\tau) + \\ &k\_3\ A(T\_1)\ \exp\ (ipT\_0)\ cos\ (\Omega\tau) - \\ &k\_4\ [A\text{^}3\ (T\_1)\ exp\ \ 〚(3ipT\_0) + \\ &3A\text{^}2\ (T\_1)\ \bar{A}(T\_1)\ exp\ (ipT\_0)〛\ ] - \\ &k\_5\ ipA(T\_1)\ exp\ (ipT\_0) + cc \end{aligned} \tag{53}$$

In which cc represents the conjugate in (53).

Primary resonance $\Omega \approx p$

We introduce the frequency parameter σ for describing the closeness of Ω top:

$$\Omega = p + \varepsilon\sigma\ , \sigma = o(1) \tag{54}$$

Substituting (54) in (53) and removing secular terms:

$$\begin{aligned} &-2ipD\_1\text{^}1\, A(T\_1) + 1/2\ k\_2\ \exp\ \ 〚 \\ &[i(\dashv 〛\ \varepsilon\sigma)\tau] - \ 3\ \ 〚k\_4\ A〛 \\ &\text{^}2\ (T\_1)\ \bar{A}(T\_1) - ik\_5\ pA(T\_1) = 0 \end{aligned} \tag{55}$$

We rewrite the function $A(T_1)$ in the polar form as follows:

$$A(T_1) = \frac{1}{2} a(T_1)\, exp[i\beta(T_1)] \tag{56}$$

In which $a(T_1)$ampluide and $\beta(T_1)$ are the phases of functions with real values. Now, by separating the real and conceptual parts in (56), the homogeneous section of the equation of the hasan unequivocal solution in Eq. (56) is solved when the solvability conditions are satisfied, and where the solvability condition is satisfied with the zero secular terms in the equation. The steady-state motion equation can be achieved by $D_1^1\theta(T_1) = 0$and$D_1^1 a(T_1) = 0$, and the frequency response equation can be written as:

$$a^2\left[k_5^2 + \left(2\sigma - \frac{3k_4 a^2}{4p}\right)^2\right] = \frac{k_2^2}{p^2} \tag{57}$$

In (57), it is clear that a is the domain and σ is the frequency parameter, k_4 is the nonlinear coefficient, k_5 is the damping factor and k_2 is the amplitude of the actuated.

Super harmonic resonance $\Omega \approx \frac{1}{3}p$

When Ω is away from p, the stimulation effect will be small. Afterwards, in comparison to the nonlinear force and the force absorbing pressure, we regarded the stimulation effect as insignificant.

$$\begin{aligned} &\ddot{S} + k_1 S = \varepsilon\big[k_3 S\, cos(\Omega\tau) - k_4 S^3 - \\ &k_5\dot{S}\big] + k_2\, cos(\Omega\tau) \end{aligned} \tag{58}$$

Solving (57) is as follows:

$$S(\tau) = Y_1(T_0, T_1) + \varepsilon Y_2(T_0, T_1) \tag{59}$$

Where $T_n = \varepsilon^n\tau, n = 0,1$. By substituting (59) in (58) then the general solution to the equation is written as follows:

$$\begin{aligned} &Y_1 = A(T_1)\, exp(ipT_0) + \\ &\Lambda\, exp(i\Omega T_0) + cc \end{aligned} \tag{60}$$

Where $\Lambda = \frac{1}{2}k_2(k_1 - \Omega^2)^{-1}$ and p^2=k_1. By Substituting Y_1 in Equation (57) we have:

$$\begin{aligned} &D_0^2 Y_2 + k_1 Y_2 = -(2ipD_1^1 A + k_5 ipA + \\ &6k_4 A\Lambda^2 + 3k_4 A^2\bar{A})\, exp(ipT_0) + \\ &\frac{1}{2}k_3\{A exp[i(p+\Omega)T_0] + \\ &\Lambda\, exp(2i\Omega T_0) + \Lambda + \bar{A}\, exp[i(\Omega - \\ &p)T_0]\} - k_4\{A^3\, exp(3ipT_0) + \\ &\Lambda^3\, exp(3i\Omega T_0) + 3A\Lambda^2 \exp[i(p + \\ &2\Omega)T_0] + 3A^2\Lambda \exp[i(p+2\Omega)T_0] + \\ &3\Lambda\bar{A}^2\, exp[i(\Omega - 2p)T_0] + \\ &3A\Lambda^2 \exp[i(p - 2\Omega)T_0]\} - (6k_4 A\bar{A}\Lambda + \\ &ik_5\Omega\Lambda + 3k_4\Lambda^3)\, exp(i\Omega T_0) + cc \end{aligned} \tag{61}$$

Here, we introduced the approximation of Ω to $\frac{1}{3}p$ with the introduction of the frequency parameter σ as follows:

$$3\Omega = p + \varepsilon\sigma\ , \sigma = o(1) \tag{62}$$

In (61) the terms corresponding to *the* exp $(\pm ipT_0)$($i\text{^}2 = -1$)and $\exp(\pm 3i\Omega T_0)$produce secular terms in Y_1. These secular classes are deleted at Y_1if:

$$\begin{aligned} &(2ipD_1^1 A + ik_5 pA + 6k_4 A\Lambda^2 + \\ &3k_4 A^2\bar{A})\, exp(ipT_0) + \\ &k_4\Lambda^3\, exp(3i\Omega T_0) = 0 \end{aligned} \tag{63}$$

Using [63] we have:

$$\begin{aligned} &D_1^1 a(T_1) = -\tfrac{k_5}{2}a(T_1) - \\ &\tfrac{k_4\Lambda^3}{p} sin\theta(T_1) D_1^1\theta(T_1) = a(T_1)\sigma - \\ &\tfrac{3k_4\Lambda^2}{p} a(T_1) - \tfrac{3k_4}{8p}a^3(T_1) - \tfrac{k_4\Lambda^3}{p} cos\theta \end{aligned} \tag{64}$$

In which $\theta(T_1) = \sigma T_1 - \beta(T_1)$. The steady-state motion of the system can be obtained by $D_1^1 a(T_1) = 0$ and $D_1^1\theta(T_1) = 0$. We can use equation (64) to obtain the frequency response for the super

harmonic resonance that can be estimated by using the following equation:

$$a^2\left[\frac{k_5^2}{4}+\left(\sigma-\frac{3k_4\Lambda^2}{p}-\frac{3k_4a^2}{8p}\right)^2\right]=\frac{k_4^2\Lambda^6}{p^2} \quad (65)$$

Subharmonic resonance $\Omega = 3p$

Examining the sub-harmonic resonance, we introduced the parameter σ:

$$\Omega = 3p+\varepsilon\sigma\,,\sigma=o(1) \quad (66)$$

For the steady-state motions corresponding to $D_1^1a(T_1)=0$ and $D_1^1\theta(T_1)=0$,$D_1^1a(T_1)=0$ and $D_1^1\theta(T_1)=0$, we obtained the frequency response equation as follows:

$$\left[\frac{9k_5^2}{4}+\left(\sigma-\frac{9k_4\Lambda^2}{p}-\frac{9k_4a^2}{8p}\right)^2\right]=\frac{81k_4^2\Lambda^2}{16p^2}a^2 \quad (67)$$

4. Numerical example

In this section, the nonlinear forced vibration of a simply supported micro beam (shown in Fig.1) was investigated.

4.1. Validation

Before presenting the results and analyzing them, we first checked the results. Here, considering $l_0=l_1=0$ and $l_2=l$, the results corresponding to the modified couple stress theory were obtained. Accordingly, the results shown on the basis of a double-headed microbeam based on the modified couple stress theory, are presented in Fig. 2. In Fig. 2, it can be observed that the results of nonlinear dynamic analysis for a microbeam were verified and closely matched the results of article [26]

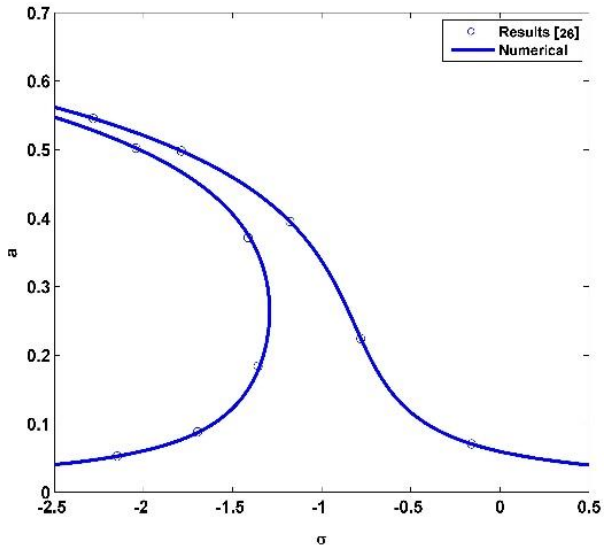

Fig. 2. Verification of the results obtained for dynamic nonlinear response

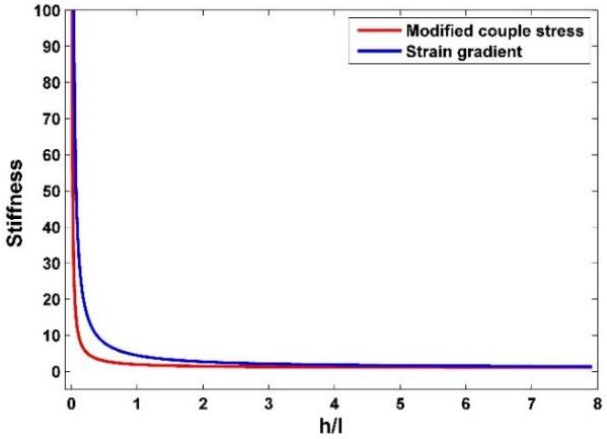

Fig. 3. Hardness ratio based on thickness variation

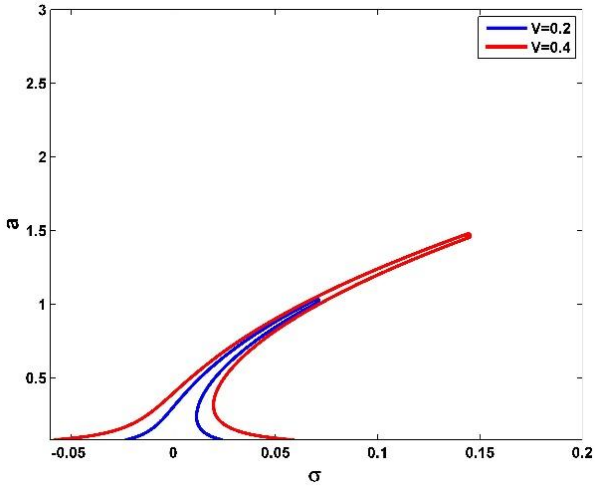

Fig. 4. Changes in excitation range by varying the applied voltage

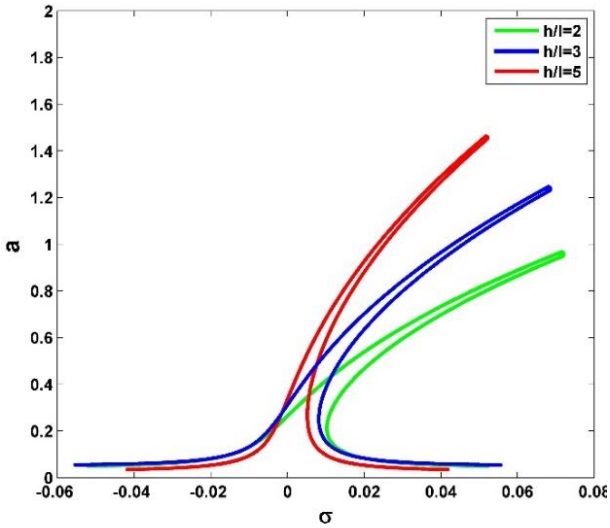

Fig. 5. Changes in primary resonance with change in thickness

Dynamic nonlinear response

Here, the length (L), width (b), height (h) of the microbeam and the gap (d) were fixed: $E_b = 169\times10^9$; $E_p = 78.6\times10^9$; $\vartheta_b = 0.06$; $\vartheta_p = 0.3$; $\rho_b = 0.06\rho_p = 7500$; $e_{31} = 9.31$; $l_b =$

17.6×10^{-6}; $l_p = 17.6 \times 10^{-6}$; $h_b = 2l_b \times 10^{-6}$; $h_b = 0.5l_p \times 10^{-6}$;$\varepsilon_0 = 8.854 \times 10^{-12}$. Furthermore, the assumption $l_0 = l_1 = l_2 = l$ was employed in the numerical simulations for the strain gradient elasticity theory.

In this paper, the dynamic response of the nonlinear system was also investigated. We analysed the effects of thickness, width and piezoelectric actuation on the system response. The main reliance on these results was made on approximate analytical methods. As can be seen in Fig. 3, linear hardness depends on the values of the h/l and the amplitude of V of the applied voltage. The hardness increased in proportion to h/l decreasing, which means that a reduction in the beam's thickness resulted in the "hardening" of the system. On the contrary, linear stiffness lessened in proportion to increasing the applied voltage, which caused the "soft" behaviour of the system.

Figure 4 shows the microbeam frequency response curve for various AC voltages, which increased with the rise in the response area V, and it also shows that the amplitude of the response increased with raising the amplitude of the actuation force. The amplitude of the oscillations and the corresponding frequency increased, which means that the increase in external actuation changed the nonlinear resonance to the higher actuation frequencies. However, it should be noted that changes in the external actuation did not change the nonlinear model. Frequency response curves showed that for small amplitudes, in the primary resonance of the system, the hardening behaviours were increased.

As shown in the fig. 4, while increasing the AC voltage, the nonlinear amplitude of the vibration was increased, and the nonlinear resonance occurred at a higher excitation frequency. On the other hand, linear stiffness decreased with increasing the applied voltage, which resulted in a more "stiffness" behaviour of the system.

Furthermore, for different thicknesses, the amplitude of the beam showed the decrease of microbeam frequencies for the primary resonance. It is obvious that the oscillation amplitude increased with increasing the scale of h/l, while the frequency response curves were reduced by decreasing h/l. These results showed that the reduction in the thickness of the microbeams increased the stiffness of the microbeam and also the nonlinearity of the microbeam. Increasing the value of h/l caused the system to soften. Also, as shown in the fig. 5, the amplitude of a nonlinear vibration increased with increasing h/l. With increasing h/l, the static deviation of the microbeam was increased. This is only due to the stiffening and hardening behaviours. We found that the system response and nonlinearity of the system increased when h/l was small.

To improve the efficiency of the system, we examined the effect of the non-uniform beam model on the frequency response. We studied the effect of the non-uniform parameter on the microbeam for two resonances. In Fig. 6 as we observe, the frequency response increased with the non-uniformity of the microbeam.

Figure 7 shows the microbeam frequency response for super harmonic resonance for various beam thicknesses. With increasing h/l, the increase of the amplitude of oscillation was obvious.

It is obvious that the frequency response curves bended to the right side by decreasing the value of h/l, which implied that decreasing the thickness of the beam increased nonlinearity. Considering different size scale h/l, the frequency of the system's response curves is plotted in Fig. 7. With an increase in h/l, it is clear that the response area widened and so the maximum amplitude of oscillations was increased.

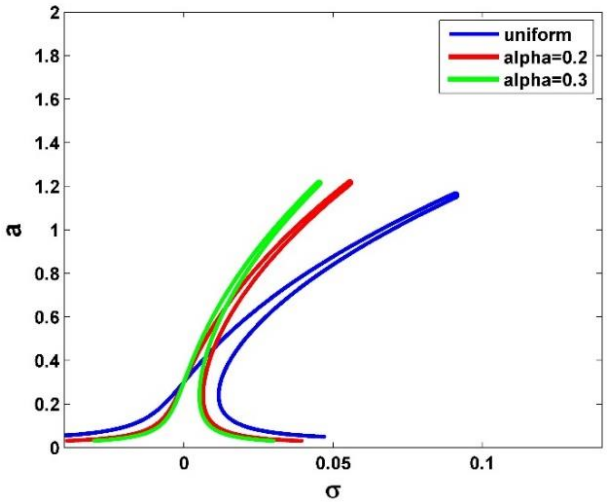

Fig. 6. Comparison of uniform and non-uniform modes

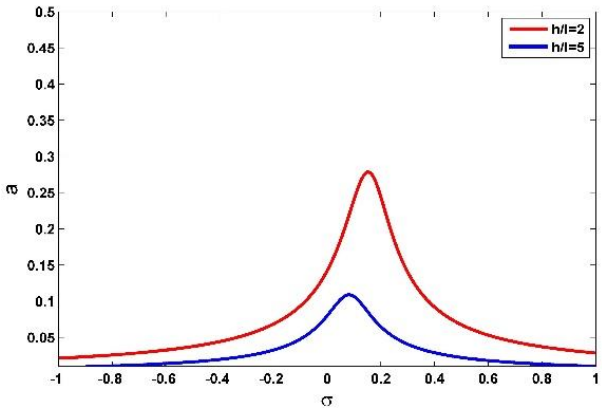

Fig. 7. Changes in excitation range by varying the applied voltage

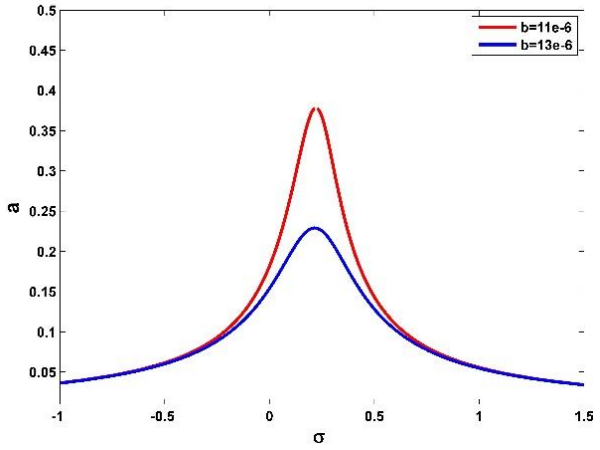

Fig. 8.Super harmonic resonance by changing the width of the beam

Figure 8 shows the effects of the b parameter on frequency response curves for the super harmonic resonance. With increasing b, it is seen that the resonance range was reduced, and the resonance zone decreased.

As shown in Fig. 9, the system frequency response curves are plotted for different sizes of h/l for the subharmonic resonance. With increasing h/l, it is clear from Fig. 9 that by increasing the thickness, the amplitude of maximum oscillations also increased. Moreover, we see that the frequency response curves were reduced by decreasing the h/l, which shows that the reduction of h/l nonlinear effect increased in the model. The effect of parameter b on the subharmonic resonance is shown in Fig. 10. By decreasing b, it is clear that the response range increased.

In fig. 11 in order to improve the results of the modelling, we investigated the effect of the non-uniform beam model on frequency responses for three resonances. As we can see, the frequency response increased with the non-uniform microbeam.

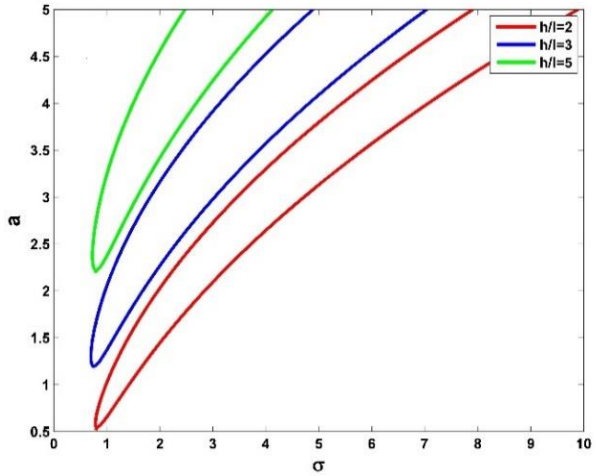

Fig. 9. Sub-harmonic resonance with the change of the thickness

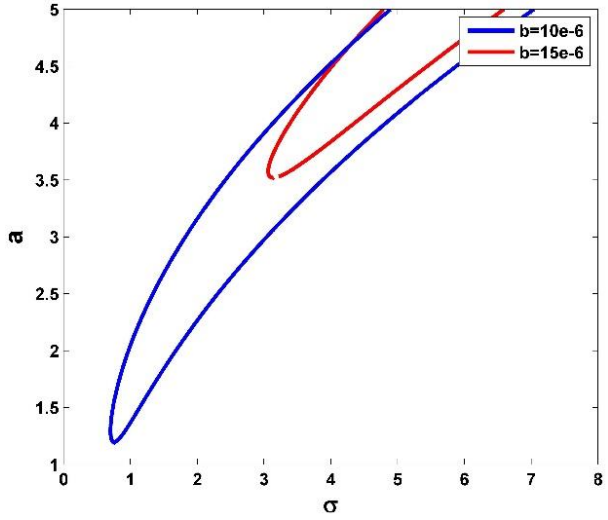

Fig. 10. The effect of b parameter on the response of sub-harmonic resonances

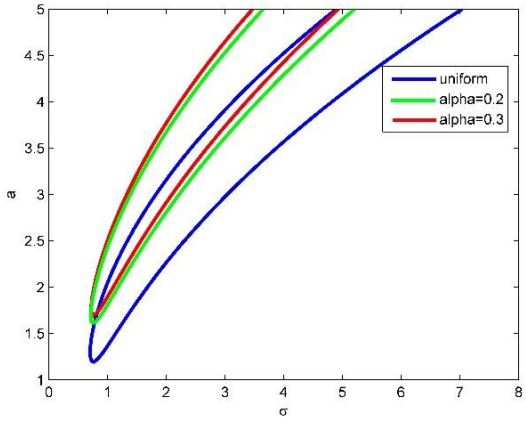

Fig. 11. Comparison of uniform and non-uniform states for the super harmonic resonance

5. Conclusions

In this research, the microbeam dynamical analysis with piezoelectric actuation was investigated. In order to model the length scale, the strain gradient theory was used, and the equations of motion and boundary conditions were obtained using Hamilton's method, and they were reduced using Galerkin's method. Also, the effect of size, thickness, and length of the microbeam and piezoelectric were considered on the system response. The results demonstrated that along with the reducing effect of size, the hardness of the microbeam increased, which implied that if the thickness of the beam was less, then it resulted in the "hardening" of the system. On the other hand, linear stiffness decreased while increasing the applied voltage, caused the "softening" behaviour of the system. It has also been shown that the microbeam frequency response was increased with an increase in voltages, which increased the amplitude of the response by elevating the amplitude of the actuation force. Finally, it is concluded that when

the thickness ratio was increased, non-classical theories evaluated the same values for the frequency as those of the classical theory. This shows that the beam based on the strain gradient theory was stronger than the beam based on the model with modified couple stress and classical theory. The results have shown that the oscillation amplitude increased with an increasing size scale, while the frequency response curves were reduced by decreasing h/l. Also, the results for different thicknesses of superharmonic and subharmonic resonance are presented here.

Appendix A

The non-dimensional of Eq. 44 can be written as:

$$\rho A \frac{d}{T^2}\frac{\partial^2 W}{\partial \tau^2} + be_{31}V_p \frac{d}{L^2}\frac{\partial^2 W}{\partial X^2} - \left(4\mu \frac{\partial^2 A(x)}{\partial^2 x} l_0^2 + \frac{8}{5}\frac{\partial^2 A(x)}{\partial^2 x} l_1^2\right)\left(\frac{d}{L}\frac{\partial W}{\partial X}\right)\left(\frac{d}{L^2}\frac{\partial^2 W}{\partial X^2}\right)\left(\frac{d}{L^3}\frac{\partial^3 W}{\partial X^3}\right) -$$
$$2\left(4\mu\left(\frac{\partial A(x)}{\partial x}\right) l_0^2 + \frac{8}{5}\mu\left(\frac{\partial A(x)}{\partial x}\right) l_1^2\right)\left(\frac{d}{L^2}\frac{\partial^2 W}{\partial X^2}\right)^2\left(\frac{d}{L^3}\frac{\partial^3 W}{\partial X^3}\right) -$$
$$2\left(4\mu\left(\frac{\partial A(x)}{\partial x}\right) l_0^2 + \frac{8}{5}\mu\left(\frac{\partial A(x)}{\partial x}\right) l_1^2\right)\left(\frac{d}{L}\frac{\partial W}{\partial X}\right)\left(\frac{d}{L^3}\frac{\partial^3 W}{\partial X^3}\right)^2 -$$
$$2\left(4\mu\left(\frac{\partial A(x)}{\partial x}\right) l_0^2 + \frac{8}{5}\mu\left(\frac{\partial A(x)}{\partial x}\right) l_1^2\right)\left(\frac{d}{L}\frac{\partial W}{\partial X}\right)\left(\frac{d}{L^2}\frac{\partial^2 W}{\partial X^2}\right)\left(\frac{d}{L^4}\frac{\partial^4 W}{\partial X^4}\right) -$$
$$3\left(4\mu A(x) l_0^2 + \frac{8}{5}\mu A(x) l_1^2\right)\left(\frac{d}{L^2}\frac{\partial^2 W}{\partial X^2}\right)\left(\frac{d}{L^3}\frac{\partial^3 W}{\partial X^3}\right)^2 -$$
$$2\left(4\mu A(x) l_0^2 + \frac{8}{5}\mu A(x) l_1^2\right)\left(\frac{d}{L^2}\frac{\partial^2 W}{\partial X^2}\right)^2\left(\frac{d}{L^4}\frac{\partial^4 W}{\partial X^4}\right) -$$
$$3\left(4\mu A(x) l_0^2 + \frac{8}{5}\mu A(x) l_1^2\right)\left(\frac{d}{L}\frac{\partial W}{\partial X}\right)\left(\frac{d}{L^3}\frac{\partial^3 W}{\partial X^3}\right)\left(\frac{d}{L^4}\frac{\partial^4 W}{\partial X^4}\right) -$$
$$\left(4\mu A(x) l_0^2 + \frac{8}{5}\mu A(x) l_1^2\right)\left(\frac{d}{L}\frac{\partial W}{\partial X}\right)\left(\frac{d}{L^2}\frac{\partial^2 W}{\partial X^2}\right)\left(\frac{d}{L^5}\frac{\partial^5 W}{\partial X^5}\right) +$$
$$\left(2\mu \frac{\partial^3 A(x)}{\partial^3 x} l_0^2 + \frac{4}{5}\frac{\partial^3 A(x)}{\partial^3 x} l_1^2\right)\left(\frac{d}{L}\frac{\partial W}{\partial X}\right)\left(\frac{d}{L^2}\frac{\partial^2 W}{\partial X^2}\right) -$$
$$3\left(2\mu \frac{\partial^2 A(x)}{\partial^2 x} l_0^2 + \frac{4}{5}\frac{\partial^2 A(x)}{\partial^2 x} l_1^2\right)\left(\frac{d}{L^2}\frac{\partial^2 W}{\partial X^2}\right)^2 -$$
$$3\left(2\mu \frac{\partial^2 A(x)}{\partial^2 x} l_0^2 + \frac{4}{5}\frac{\partial^2 A(x)}{\partial^2 x} l_1^2\right)\left(\frac{d}{L}\frac{\partial W}{\partial X}\right)\left(\frac{d}{L^3}\frac{\partial^3 W}{\partial X^3}\right) -$$
$$9\left(2\mu\left(\frac{\partial A(x)}{\partial x}\right) l_0^2 + \frac{4}{5}\mu\left(\frac{\partial A(x)}{\partial x}\right) l_1^2\right)\left(\frac{d}{L^2}\frac{\partial^2 W}{\partial X^2}\right)\left(\frac{d}{L^3}\frac{\partial^3 W}{\partial X^3}\right) -$$
$$3\left(2\mu\left(\frac{\partial A(x)}{\partial x}\right) l_0^2 + \frac{4}{5}\mu\left(\frac{\partial A(x)}{\partial x}\right) l_1^2\right)\left(\frac{d}{L}\frac{\partial W}{\partial X}\right)\left(\frac{d}{L^4}\frac{\partial^4 W}{\partial X^4}\right) -$$
$$3\left(2\mu A(x) l_0^2 + \frac{4}{5}\mu A(x) l_1^2\right)\left(\frac{d}{L^3}\frac{\partial^3 W}{\partial X^3}\right)^2 - 4\left(2\mu A(x) l_0^2 + \frac{4}{5}\mu A(x) l_1^2\right)\left(\frac{d}{L^2}\frac{\partial^2 W}{\partial X^2}\right)\left(\frac{d}{L^4}\frac{\partial^4 W}{\partial X^4}\right) - \left(2\mu A(x) l_0^2 + \frac{4}{5}\mu A(x) l_1^2\right)\left(\frac{d}{L}\frac{\partial W}{\partial X}\right)\left(\frac{d}{L^5}\frac{\partial^5 W}{\partial X^5}\right) + \left(E\frac{\partial^2 I(x)}{\partial^2 x} + 2\mu \frac{\partial^2 A(x)}{\partial^2 x} l_0^2 + \frac{8}{15}\mu \frac{\partial^2 A(x)}{\partial^2 x} l_1^2 + \mu \frac{\partial^2 A(x)}{\partial^2 x} l_2^2\right)\left(\frac{d}{L^2}\frac{\partial^2 W}{\partial X^2}\right) + 2\left(E\frac{\partial I(x)}{\partial x} + 2\mu\left(\frac{\partial A(x)}{\partial x}\right) l_0^2 + \frac{8}{15}\mu\left(\frac{\partial A(x)}{\partial x}\right) l_1^2 + \mu\left(\frac{\partial A(x)}{\partial x}\right) l_2^2\right)\left(\frac{d}{L^3}\frac{\partial^3 W}{\partial X^3}\right) + \left(EI(x) + 2\mu A(x) l_0^2 + \frac{8}{15}\mu A(x) l_1^2 + \mu A(x) l_2^2\right)\left(\frac{d}{L^4}\frac{\partial^4 W}{\partial X^4}\right) - \left(2\mu\left(\frac{\partial^3}{\partial x^3} I(x)\right) l_0^2 + \frac{4}{5}\mu\left(\frac{\partial}{\partial x^3} I(x)\right) l_1^2\right)\left(\frac{d}{L^3}\frac{\partial^3 W}{\partial X^3}\right) - 3\left(2\mu\left(\frac{\partial^2}{\partial x^2} I(x)\right) l_0^2 + \frac{4}{5}\mu\left(\frac{\partial^2}{\partial x^2} I(x)\right) l_1^2\right)\left(\frac{d}{L^4}\frac{\partial^4 W}{\partial X^4}\right) - 3\left(2\mu\left(\frac{\partial}{\partial x} I(x)\right) l_0^2 + \frac{4}{5}\mu\left(\frac{\partial}{\partial x} I(x)\right) l_1^2\right)\left(\frac{d}{L^5}\frac{\partial^5 W}{\partial X^5}\right) - \left(2\mu I(x) l_0^2 + \frac{4}{5}\mu I(x) l_1^2\right)\left(\frac{d}{L^6}\frac{\partial^6 W}{\partial X^6}\right) - \frac{1}{2}E\left(\frac{\partial}{\partial x} A(x)\right)\left(\frac{d}{L}\frac{\partial W}{\partial X}\right)^3 - \frac{3}{2}EA(x)\left(\frac{d}{L}\frac{\partial W}{\partial X}\right)^2\left(\frac{d}{L^2}\frac{\partial^2 W}{\partial X^2}\right) + p = 0$$

References

[1] T. Galchev, H. Kim, and K. Najafi, "Micro power generator for harvesting low-frequency and nonperiodic vibrations," Journal of Microelectromechanical Systems, vol. 20, pp. 852-866, 2011.

[2] S. P. Beeby, M. J. Tudor, and N. White, "Energy harvesting vibration sources for microsystems applications," Measurement science and technology, vol. 17, p. R175, 2006.

[3] S. Beeby, G. Ensel, N. M. White, and M. Kraft, MEMS mechanical sensors: Artech House, 2004.

[4] S. Roundy, P. K. Wright, and J. Rabaey, "A study of low level vibrations as a power source for wireless sensor nodes," Computer communications, vol. 26, pp. 1131-1144, 2003.

[5] M. I. Younis, E. M. Abdel-Rahman, and A. Nayfeh, "A reduced-order model for electrically actuated microbeam-based MEMS," Journal of Microelectromechanical systems, vol. 12, pp. 672-680, 2003.

[6] E. M. Abdel-Rahman, M. I. Younis, and A. H. Nayfeh, "A nonlinear reduced-order model for electrostatic MEMS," in ASME 2003 International Design Engineering Technical Conferences and Computers and Information in Engineering Conference, 2003, pp. 1771-1778.

[7] A. R. Kivi, S. Azizi, and P. Norouzi, "Bifurcation analysis of an electrostatically actuated nano-beam based on modified couple stress theory," Sensing and Imaging, vol. 18, p. 32, 2017.

[8] M. H. Ghayesh, H. Farokhi, and M. Amabili, "Nonlinear behaviour of electrically actuated MEMS resonators," International Journal of Engineering Science, vol. 71, pp. 137-155, 2013.

[9] A. G. Arani, M. Abdollahian, and R. Kolahchi, "Nonlinear vibration of a nanobeam elastically bonded with a piezoelectric nanobeam via strain

gradient theory," International Journal of Mechanical Sciences, vol. 100, pp. 32-40, 2015.

[10] R. Ansari, M. Ashrafi, and S. Hosseinzadeh, "Vibration characteristics of piezoelectric microbeams based on the modified couple stress theory," Shock and Vibration, vol. 2014, 2014.

[11] S. M. Hosseini, A. Shooshtari, H. Kalhori, and S. N. Mahmoodi, "Nonlinear-forced vibrations of piezoelectrically actuated viscoelastic cantilevers," Nonlinear Dynamics, vol. 78, pp. 571-583, 2014.

[12] S. Azizi, M. T. Chorsi, and F. Bakhtiari-Nejad, "On the secondary resonance of a MEMS resonator: A conceptual study based on shooting and perturbation methods," International Journal of Non-Linear Mechanics, vol. 82, pp. 59-68, 2016.

[13] F. C. Yazdi and A. Jalali, "Vibration behavior of a viscoelastic composite microbeam under simultaneous electrostatic and piezoelectric actuation," Mechanics of Time-Dependent Materials, vol. 19, pp. 277-304, 2015.

[14] H. Madinei, H. H. Khodaparast, S. Adhikari, M. Friswell, and M. Fazeli, "Adaptive tuned piezoelectric MEMS vibration energy harvester using an electrostatic device," The European Physical Journal Special Topics, vol. 224, pp. 2703-2717, 2015.

[15] A. K. Hoshiar and H. Raeisifard, "A study of the nonlinear primary resonances of a micro-system under electrostatic and piezoelectric excitations," Proceedings of the Institution of Mechanical Engineers, Part C: Journal of Mechanical Engineering Science, vol. 229, pp. 1904-1917, 2015.

[16] R. A. Toupin, "Elastic materials with couple-stresses," Archive for Rational Mechanics and Analysis, vol. 11, pp. 385-414, 1962.

[17] S. Zhou and Z. Li, "Length scales in the static and dynamic torsion of a circular cylindrical micro-bar," 2001.

[18] M. Asghari, M. Kahrobaiyan, M. Rahaeifard, and M. Ahmadian, "Investigation of the size effects in Timoshenko beams based on the couple stress theory," Archive of Applied Mechanics, vol. 81, pp. 863-874, 2011.

[19] F. Yang, A. Chong, D. C. C. Lam, and P. Tong, "Couple stress based strain gradient theory for elasticity," International Journal of Solids and Structures, vol. 39, pp. 2731-2743, 2002.

[20] J. Hutchinson and N. Fleck, "Strain gradient plasticity," in Advances in applied mechanics. vol. 33, ed: Academic, 1997, pp. 295-361.

[21] D. C. Lam, F. Yang, A. Chong, J. Wang, and P. Tong, "Experiments and theory in strain gradient elasticity," Journal of the Mechanics and Physics of Solids, vol. 51, pp. 1477-1508, 2003.

[22] M. H. Kahrobaiyan, M. Asghari, M. Hoore, and M. T. Ahmadian, "Nonlinear size-dependent forced vibrational behavior of microbeams based on a non-classical continuum theory," Journal of Vibration and Control, vol. 18, pp. 696-711, 2012.

[23] M. I. Younis and A. Nayfeh, "A study of the nonlinear response of a resonant microbeam to an electric actuation," Nonlinear Dynamics, vol. 31, pp. 91-117, 2003.

[24] J. Reddy, "Microstructure-dependent couple stress theories of functionally graded beams," Journal of the Mechanics and Physics of Solids, vol. 59, pp. 2382-2399, 2011.